Available online at www.sciencedirect.com
ScienceDirect
International Journal of Heat and Mass Transfer 51 (2008) 661–671
International Journal of HEAT and MASS TRANSFER
www.elsevier.com/locate/ijhmt

Theoretical analysis of convective heat transfer of Oldroyd-B fluids in a curved pipe

Mingkan Zhang *, Xinrong Shen, Jianfeng Ma, Benzhao Zhang

Institute of Fluid Engineering, Zhejiang University, Hangzhou 310027, China

Received 30 May 2006; received in revised form 20 March 2007
Available online 17 July 2007

Abstract

Perturbation methods are used to study steady, fully developed flow of Oldroyd-B fluids through a curved pipe of circular cross-section. A perturbation solution up to secondary order is obtained for a small value of curvature ratio. The range of validity of the perturbation method are discussed and chosen carefully. Variations of temperature distribution with *Re* and *We* are discussed in detail in order to investigate the combined effects of the two parameters on temperature distribution. Present studies also show the variations of the heat transfer rate with *Re* and *We*. This study explores many new characteristics of convective heat transfer of a kind of viscoelastic fluid through curved pipes.

Keywords: Convective heat transfer; Oldroyd-B fluid; Perturbation method; Pipe flow

1. Introduction

In this paper, perturbation solutions for heat transfer of viscoelastic fluids in curved pipes are obtained. It is assumed that the fluid flow is steady, hydrodynamically and thermally fully developed, both the wall heat flux and the peripheral wall temperature of one cross-section are uniform (different wall temperature in different cross-section), and, the viscous dissipation is negligible.

Since the initial work by Dean [1,2], more and more attentions have been paid to the mass and heat transfer of Newtonian fluid through curved pipes, not only because of its practical importance in various industrial applications, but also because of physically interesting phenomena caused by the curvature of the pipe. The previous works on heat transfer concerned on the planar curved pipes with a circle cross-section, such as Akiyama and Cheng [3], Patanker et al. [4] and Yang and Chang [5]. Such works indicated that both the efficiencies of convective heat transfer and Nusselt number in curved pipes are much greater than those in straight pipes. Then Garimella and Chdrards [6] investigated the forced convective heat transfer in coiled annular ducts experimentally.

By using numerical method, Yang and Ebadian [7,8] and Choi and Park [9] studied the heat transfer and mixed convection flow in a curved annular-sector duct, respectively. More recently, Chen and Zhang [10,11] extended the former work to the heat transfer in a rotating helical pipe.

Besides Newtonian fluid, Viscoelastic fluids are also widely used in industries. Lots of industrial materials fall into this category, such as solutions and melts of polymers, soap and cellulose solutions, biological solutions, various colloids and also paints, tars, asphalts and glues. The Oldroyd-B model can be found frequently in the field of blowing and extrusion molding as well. However, it's rather surprising to find that, despite its important applications, the flow and heat transfer of viscoelastic fluids in pipes has received much less attention in the monographs than its Newtonian counterpart. Robertson and Muller [12] and Jitchote and Robertson [13] presented the perturbation solutions of flow of Oldroyd-B fluid and second order fluid,

* Corresponding author. Tel.: +86 571 87953220.
E-mail address: wangtwo@zju.edu.cn (M. Zhang).

0017-9310/$ - see front matter © 2007 Elsevier Ltd. All rights reserved.
doi:10.1016/j.ijheatmasstransfer.2007.04.040

Nomenclature

a	radius of the circle cross-section
D	symmetric part of the velocity gradient
$\boldsymbol{e}_r$, $\boldsymbol{e}_\phi$, $\boldsymbol{e}_s$	unit base vectors of the convected coordinates system
$\boldsymbol{e}_1$, $\boldsymbol{e}_2$, $\boldsymbol{e}_3$	unit base vectors of the Cartesian coordinate system
G	axial gradient of w, $G = \partial w/\partial s$
H	axial gradient of T, $H = \partial T/\partial s$
p	pressure
Pr	Prandtl number, $Pr = \eta/\alpha$
Pe	Peclet number, $Pe = RePr$
R	curvature radius
Re	Reynolds number, $Re = \rho a W_0/\eta$
r	radial direction coordinates
s	axial direction coordinates
T, T_w	temperature of fluid and wall
T_b	bulk temperature, $T_b = \int_0^1 \int_0^{2\pi} Twr\,d\phi\,dr / \int_0^1 \int_0^{2\pi} wr\,d\phi\,dr$
T_0	characteristic temperature, $T_0 = aPrH$
$\boldsymbol{u}$	vector of velocity
u, v, w	physical velocity components
W_0	characteristic temperature, $W_0 = Ga^2/4\eta$
We	Weissenberg number, $\lambda W_0/a$

Greek symbols

α	thermal diffusivity
η_s, η_p	solvent viscosity and polymeric contribution to the viscosity
η	sum of η_s and η_p
κ	curvature ratio
λ	relax time
ρ	density of the fluid
$\boldsymbol{\tau}$	extra stress tensor
ϕ	angular coordinate
ψ	stream function

Subscripts and superscripts

$*$	dimensional variable
max	maximum value
∇	upper-convected derivative

respectively. Almost at the same time, Fan et al. [14] investigated the comparison between fully developed viscous and viscoelastic flows in curved pipes by using finite element method. In their work, they investigated not only the flow characteristics but the two normal stress differences as well. In the field of heat transfer of viscoelastic fluids, Cho and Harnett [15] analyzed heat transfer of polyacrylamide in Chicago tap water. Then Toh and Ghajar [16] reported thermal entrance region Nusselt values for turbulent flow of two different polyacrylamides in circular tubes experimentally. Recently, Pinho and Oliveira [17] got the analytic solution for forced convection of Phan-Thien–Tanner fluid in straight pipes.

In present work, we have extended the previous analysis of Robertson and Muller to the convective heat transfer problem of fully-developed flow of an Oldroyd-B fluid in a curved pipe. It's quite necessary and useful to investigate this problem. Besides the industrial applications, perturbation solutions of present work can provide valuable tests for the numerical simulation of heat transfer of viscoelastic fluids. Moreover, it is much easier to analyze perturbation solutions than numerical ones. In this paper, the combined effects of viscosity, centrifugal force and elasticity on heat transfer are examined in detail. Many new and interesting conclusions are drawn.

2. Governing equations

The momentum and constitutive equations of present work are from reference to the work of Robertson and Muller. We consider the incompressible Oldroyd-B fluids, for which the extra stress tensor τ^* can be written as

$$\boldsymbol{\tau}^* = \boldsymbol{\tau}^{s*} + \boldsymbol{\tau}^{p*}, \tag{1}$$

where $\boldsymbol{\tau}^{s*}$ and $\boldsymbol{\tau}^{p*}$ are defined as

$$\boldsymbol{\tau}^{s*} = 2\eta_s \boldsymbol{D}^*, \quad \boldsymbol{\tau}^{p*} + \lambda \overset{\nabla}{\boldsymbol{\tau}}{}^{p*} = 2\eta_p \boldsymbol{D}^*. \tag{2}$$

In Eq. (2), η_s, η_p and λ are referred to as the solvent viscosity, polymeric contribution to the viscosity and polymer relaxation time, respectively. The rate of deformation tensor, $\boldsymbol{D}^*$, is the symmetric part of the velocity gradient. The components of $\boldsymbol{D}^*$ relative to a rectangular coordinate system are

$$D^*_{ij} = \frac{1}{2}\left(\frac{\partial v^*_i}{\partial x^*_j} + \frac{\partial v^*_j}{\partial x^*_i}\right). \tag{3}$$

The "∇" notation introduced in (2) denotes the upper-convected derivative, which for an arbitrary second-order tensor $\boldsymbol{S}^*$ with coordinates $\boldsymbol{S}^*_{ij}$ relative to a rectangular coordinate system, is

$$\overset{\nabla}{\boldsymbol{S}}{}^*_{ij} = \frac{\partial \boldsymbol{S}^*_{ij}}{\partial t^*} + v^*_k \frac{\partial \boldsymbol{S}^*_{ij}}{\partial x^*_k} - \frac{\partial v^*_i}{\partial x^*_k}\boldsymbol{S}^*_{kj} - \boldsymbol{S}^*_{ik}\frac{\partial v^*_j}{\partial x^*_k}. \tag{4}$$

In the limit of λ equal to zero, the Oldroyd-B equation reduces to the Newtonian constitutive equation and for vanishing η_s to the upper-convected Maxwell constitutive equation.

Fig. 1 shows the curved pipe and the convected coordinates system (r^*, ϕ, s^*) used in present work. R is the radius of curvature of the pipe and a the radius of the circle cross-section. $\boldsymbol{e}_r$, $\boldsymbol{e}_\phi$, $\boldsymbol{e}_s$ are the unit base vectors of the convected coordinates system (r^*, ϕ, s^*) defined relative to the unit base vectors of the Cartesian coordinate system $\boldsymbol{e}_1$, $\boldsymbol{e}_2$, $\boldsymbol{e}_3$ as

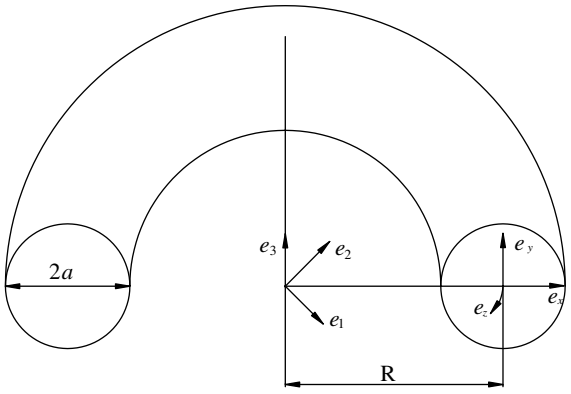

Fig. 1. The curved pipe and the coordinate system.

$$\begin{aligned}
\boldsymbol{e}_r &= \cos\phi\left(\cos\frac{\tilde{s}}{R}\boldsymbol{e}_1 + \sin\frac{\tilde{s}}{R}\boldsymbol{e}_2\right) + \sin\phi\boldsymbol{e}_3,\\
\boldsymbol{e}_\phi &= -\sin\phi\left(\cos\frac{\tilde{s}}{R}\boldsymbol{e}_1 + \sin\frac{\tilde{s}}{R}\boldsymbol{e}_2\right) + \cos\phi\boldsymbol{e}_3\\
\boldsymbol{e}_s &= \sin\frac{\tilde{s}}{R}\boldsymbol{e}_1 - \cos\frac{\tilde{s}}{R}\boldsymbol{e}_2.
\end{aligned} \tag{5}$$

The non-dimensional quantities are introduced as following:

$$\begin{aligned}
&s = \frac{s^*}{a}, \quad r = \frac{r^*}{a},\\
&(u,v,w) = \frac{(\boldsymbol{u}^*\cdot\boldsymbol{e}_r, \boldsymbol{u}^*\cdot\boldsymbol{e}_\phi, \boldsymbol{u}^*\cdot\boldsymbol{e}_s)}{W_o}, \quad p = \frac{ap^*}{\eta W_o},\\
&\boldsymbol{\tau}^s = \frac{a}{\eta W_o}\boldsymbol{\tau}^{s*}, \quad \boldsymbol{\tau}^p = \frac{a}{\eta W_o}\boldsymbol{\tau}^{p*}, \quad T = \frac{T_w - T^*}{T_o}
\end{aligned} \tag{6}$$

where $\boldsymbol{u}^*$ is the velocity vector of the flow, η the sum of η_p and η_s, T_w the temperature on the wall of one cross-section of the pipe, W_o and T_o the characteristic velocity and the characteristic temperature of the flow, respectively. By definition of a hydrodynamically and thermally fully developed flow in curved pipes, the pumping power of flow $\partial p^*/\partial s^*$ and the heat flux $\partial T^*/\partial s^*$ are constants denoted as $-G$ and H. So the characteristic velocity and the characteristic temperature are defined as follows:

$$\begin{aligned}
&W_o = \frac{a^2}{4\eta}\left(-\frac{\partial p^*}{\partial s^*}\right) = \frac{Ga^2}{4\eta},\\
&T_o = RePra\frac{\partial T^*}{\partial s^*} = RePraH,
\end{aligned} \tag{7}$$

where Pr called Prandtl number, is the ratio of η/ρ and the thermal diffusivity α.

The rest non-dimensional parameters used in present work are including, the curvature ratio, κ, the Reynolds number, Re, the Weissenberg number, We, the Peclet number, Pe, and the ratio of the polymeric to total shear viscosity,

$$\begin{aligned}
&\kappa = \frac{a}{R}, \quad Re = \frac{\rho W_o a}{\eta}, \quad We = \frac{\lambda W_o}{a},\\
&Pe = RePr, \quad \frac{\eta_p}{\eta}
\end{aligned} \tag{8}$$

where ρ is the constant density of the fluid.

Generally speaking, for the problems of incompressible fully developed flow, a non-dimensional stream function ψ can be introduced to avoid the troubles from pressure. With respect to ψ, velocities u and v can be written as

$$u = -\frac{1}{rM}\frac{\partial\psi}{\partial\phi}, \quad v = \frac{1}{M}\frac{\partial\psi}{\partial r}, \tag{9}$$

where

$$M = 1 + \kappa x. \tag{10}$$

By using the tensor analysis from many references to the Bolinder's work [18], the continuity, momentum and energy equations for the convected coordinates system with respect to ψ are as follows:

$$\frac{\partial u}{\partial r} + \frac{1}{r}\frac{\partial v}{\partial\phi} + \left(\frac{1}{r} + \frac{\kappa\cos\phi}{M}\right)u - \frac{\kappa\sin\phi}{M}v = 0, \tag{11}$$

$$\begin{aligned}
&Re\left[\frac{1}{rM}\left(\frac{\partial\psi}{\partial r}\frac{\partial w}{\partial\phi} - \frac{\partial\psi}{\partial\phi}\frac{\partial w}{\partial r}\right) - \kappa\frac{w}{M^2}\left(\frac{\partial\psi}{\partial r}\sin\phi + \frac{1}{r}\frac{\partial\psi}{\partial\phi}\cos\phi\right)\right]\\
&\quad = \frac{4}{M} + \frac{\partial\tau_{rs}}{\partial r} + \frac{1}{r}\frac{\partial\tau_{\phi s}}{\partial\phi} + \frac{\tau_{rs}}{r} + \frac{2\kappa}{M}(\tau_{rs}\cos\phi - \tau_{\phi s}\sin\phi),
\end{aligned} \tag{12}$$

$$\begin{aligned}
&Re\left[-2\frac{\kappa w}{M}\left(r\frac{\partial w}{\partial r}\sin\phi + \frac{\partial w}{\partial\phi}\cos\phi\right)\right.\\
&\quad + \frac{1}{M^2}\left(-\frac{\partial\psi}{\partial r}\frac{\partial^3\psi}{\partial r^2\partial\phi} + \frac{\partial\psi}{\partial\phi}\frac{\partial^3\psi}{\partial r^3} + \frac{1}{r}\left(\frac{\partial^2\psi}{\partial r^2}\frac{\partial\psi}{\partial\phi} - \frac{\partial^2\psi}{\partial r\partial\phi}\frac{\partial\psi}{\partial r}\right)\right.\\
&\quad \left. + \frac{1}{r^2}\left(\frac{\partial^3\psi}{\partial r\partial\phi^2}\frac{\partial\psi}{\partial\phi} - \frac{\partial^3\psi}{\partial\phi^3}\frac{\partial\psi}{\partial r} - \frac{\partial\psi}{\partial\phi}\frac{\partial\psi}{\partial r}\right) - \frac{2}{r^3}\frac{\partial^2\psi}{\partial\phi^2}\frac{\partial\psi}{\partial\phi}\right)\\
&\quad + \frac{\kappa}{M^3}\left(\sin\phi\left(-2r\frac{\partial^2\psi}{\partial r^2}\frac{\partial\psi}{\partial r} + 3\left(\frac{\partial\psi}{\partial r}\right)^2 + \frac{1}{r}\frac{\partial\psi}{\partial\phi}\frac{\partial^2\psi}{\partial r\partial\phi}\right.\right.\\
&\quad \left. - \frac{3}{r}\frac{\partial\psi}{\partial r}\frac{\partial^2\psi}{\partial\phi^2} - \frac{1}{r^2}\left(\frac{\partial\psi}{\partial\phi}\right)^2\right) + \cos\phi\left(\frac{\partial^2\psi}{\partial r\partial\phi}\frac{\partial\psi}{\partial r} - 3\frac{\partial^2\psi}{\partial r^2}\frac{\partial\psi}{\partial\phi}\right.\\
&\quad \left.\left. - \frac{3}{r}\frac{\partial\psi}{\partial r}\frac{\partial\psi}{\partial\phi} - \frac{1}{r^2}\frac{\partial\psi}{\partial\phi}\frac{\partial^2\psi}{\partial\phi^2}\right)\right)\\
&\quad \left. + \frac{3\kappa^2}{M^4}\left(\cos^2\phi\frac{\partial\psi}{\partial r}\frac{\partial\psi}{\partial\phi} - \frac{\sin^2\phi}{2}\left(\frac{1}{r}\left(\frac{\partial\psi}{\partial\phi}\right)^2 - r\left(\frac{\partial\psi}{\partial r}\right)^2\right)\right)\right]\\
&\quad = \frac{\partial^2\tau_{rr}}{\partial r\partial\phi} - 3\frac{\partial\tau_{r\phi}}{\partial r} - r\frac{\partial^2\tau_{r\phi}}{\partial r^2} - \frac{\partial^2\tau_{\phi\phi}}{\partial r\partial\phi}\\
&\quad + \frac{1}{r}\left(\frac{\partial^2\tau_{r\phi}}{\partial\phi^2} + \frac{\partial\tau_{rr}}{\partial\phi} - \frac{\partial\tau_{\phi\phi}}{\partial\phi\partial\phi}\right)\\
&\quad - \frac{\kappa}{M}\left(\sin\phi\left(\frac{\partial\tau_{r\phi}}{\partial\phi} + \tau_{rr} + r\frac{\partial\tau_{ss}}{\partial r} - r\frac{\partial\tau_{\phi\phi}}{\partial r} - \tau_{\phi\phi}\right)\right.\\
&\quad \left. + \cos\phi\left(2\tau_{r\phi} + r\frac{\partial\tau_{r\phi}}{\partial r}\frac{\partial\tau_{ss}}{\partial\phi} - \frac{\partial\tau_{rr}}{\partial\phi}\right)\right)\\
&\quad + \frac{\kappa^2 r}{M^2}\left(\tau_{r\phi}\cos 2\phi - \frac{1}{2}(\tau_{\phi\phi} - \tau_{rr})\sin 2\phi\right),
\end{aligned} \tag{13}$$

$$-\frac{1}{rM}\frac{\partial\psi}{\partial\phi}\frac{\partial T}{\partial r}+\frac{1}{rM}\frac{\partial\psi}{\partial r}\frac{\partial T}{\partial\phi}-\frac{w}{PrM}$$
$$=\frac{1}{PrRe}\left(\frac{\partial^2 T}{\partial r^2}+\frac{1}{r^2}\frac{\partial^2 T}{\partial\phi^2}+\left(\frac{1}{r}+\frac{\kappa\cos\phi}{M}\right)\frac{\partial T}{\partial r}-\frac{\kappa\sin\phi}{M}\frac{1}{r}\frac{\partial T}{\partial\phi}\right). \tag{14}$$

The equations of the extra stress tensor are in the Appendix A.

The velocity is prescribed to be zero on the wall of the pipes. Using Eq. (9), the boundary conditions of the momentum equations are written as

$$w=0,\quad \psi=u=v=0,\quad \partial\psi/\partial r=0,$$
$$\partial\psi/\partial\phi=0,\quad \text{at } r=1. \tag{15}$$

For the non-dimensional temperature in Eq. (6), the boundary condition of energy equation is introduced as follow:

$$T=0,\quad \text{at } r=1. \tag{16}$$

3. Perturbation solution

A perturbation method is used to study heat transfer in curved pipes with circle cross-section. The perturbation parameter of present work is the curvature ratio, κ. In the limit of κ equal to zero, the heat transfer in a straight pipe is approached.

We look for the perturbation solutions for Eqs. (11)–(14) of the form

$$w=\sum_{n=0}^{\infty}\kappa^n w^{(n)},\quad \psi=\kappa\sum_{n=0}^{\infty}\kappa^n\psi^{(n+1)},\quad T=\sum_{n=0}^{\infty}\kappa^n T^{(n)}$$
$$\boldsymbol{\tau}=\sum_{n=0}^{\infty}\kappa^n\boldsymbol{\tau}^{(n)},\quad \boldsymbol{\tau}^{\mathrm{p}}=\sum_{n=0}^{\infty}\kappa^n\boldsymbol{\tau}^{p(n)},\quad \boldsymbol{\tau}^{\mathrm{s}}=\sum_{n=0}^{\infty}\kappa^n\boldsymbol{\tau}^{s(n)}. \tag{17}$$

The boundary conditions with respect to $w^{(n)}$, $\psi^{(n)}$ and $T^{(n)}$ are as follows:

$$w^{(n)}=\psi^{(n+1)}=T^{(n)}=\partial\psi^{(n+1)}/\partial r=\partial\psi^{(n+1)}/\partial\phi=0. \tag{18}$$

From the work of Robertson and Muller, we obtain the perturbation solutions of w and ψ. After substituting the perturbation solutions of w and ψ in Eq. (14) and collecting terms of κ^0, we obtain the equation respect to $T^{(0)}$ as

$$\nabla^2 T^{(0)}=-(1-r^2), \tag{19}$$

where $\nabla^2 T^{(0)}$ is given by,

$$\nabla^2 T^{(0)}=\frac{\partial^2 T^{(0)}}{\partial r^2}+\frac{1}{r}\frac{\partial T^{(0)}}{\partial r}+\frac{1}{r}\frac{\partial^2 T^{(0)}}{\partial\phi^2}. \tag{20}$$

The solution of Eq. (19) which satisfies boundary condition (18) is

$$T^{(0)}=\frac{1}{16}(r^4-4r^2+3), \tag{21}$$

which denotes the temperature distribution in straight pipes.

Then substituting Eq. (21) to (14), associated with perturbation solutions of w and ψ, and collecting terms of order κ^1, the following equation for $T^{(1)}$ can be obtained,

$$\nabla^2 T^{(1)}=\cos\phi\left[\left(\frac{9}{4}r-2r^3\right)+Re^2\left(-\frac{19}{11520}r+\frac{1}{288}r^3-\frac{1}{384}r^5+\frac{1}{1152}r^7-\frac{1}{11520}r^9\right)\right.$$
$$+We\frac{\eta_{\mathrm{p}}}{\eta}Re\left(-\frac{11}{288}r+\frac{1}{12}r^3-\frac{1}{18}r^5+\frac{1}{96}r^7\right)$$
$$\left.+\left(We\frac{\eta_{\mathrm{p}}}{\eta}\right)^2\left(-\frac{1}{6}r+\frac{1}{3}r^3-\frac{1}{6}r^5\right)\right]$$
$$+Pr\cos\phi Re\left[Re\left(-\frac{1}{144}r+\frac{11}{576}r^3-\frac{7}{384}r^5+\frac{1}{144}r^7-\frac{1}{1152}r^9\right)+We\frac{\eta_{\mathrm{p}}}{\eta}\left(-\frac{1}{24}r+\frac{5}{48}r^3-\frac{1}{12}r^5+\frac{1}{48}r^7\right)\right]. \tag{22}$$

The solution of Eq. (22) which satisfies boundary condition (18) is of the form $T^{(1)}=g_1(r)\cos\phi$ with

$$g_1(r)=\left(-\frac{19}{96}r+\frac{9}{32}r^3-\frac{1}{12}r^5\right)+Re^2\left(\frac{73}{691200}r-\frac{19}{92160}r^3+\frac{1}{6912}r^5-\frac{1}{18432}r^7+\frac{1}{92160}r^9-\frac{1}{1382400}r^{11}\right)$$
$$+We\frac{\eta_{\mathrm{p}}}{\eta}Re\left(\frac{161}{69120}r-\frac{11}{2304}r^3+\frac{1}{288}r^5-\frac{1}{864}r^7+\frac{1}{7680}r^9\right)+\left(We\frac{\eta_{\mathrm{p}}}{\eta}\right)^2\left(\frac{1}{96}r-\frac{1}{48}r^3+\frac{1}{72}r^5-\frac{1}{288}r^7\right)$$
$$+Pr\left[Re^2\left(\frac{103}{276480}r-\frac{1}{1152}r^3+\frac{11}{13824}r^5-\frac{7}{18432}r^7+\frac{1}{11520}r^9-\frac{1}{138240}r^{11}\right)\right.$$
$$\left.+We\frac{\eta_{\mathrm{p}}}{\eta}Re\left(\frac{3}{1280}r-\frac{1}{192}r^3+\frac{5}{1152}r^5-\frac{1}{576}r^7+\frac{1}{3840}r^9\right)\right]. \tag{23}$$

The higher-order terms in the series solution can be obtained using procedures similar to those used to calculate $T^{(0)}$ and $T^{(1)}$. As for the curved pipe solution for Newtonian fluid, $T^{(2)}$ can be written as $T^{(2)}=g_2(r)+\cos(2\phi)g_3(r)$. The solution for $T^{(2)}$ is in Appendix B.

4. Results and discussion

Combined effects of viscosity, centrifugal force and elasticity on the flow of viscoelastic fluids make the heat transfer in curved pipes very complicated. Our work focuses on the convective heat transfer in curved pipes and the results in the paper will almost be confined to the case of $Pr=0.85$.

4.1. Temperature distribution

Fig. 2 presents the distributions of different order solutions of temperature for different *Re*. In this and other figures, the left half of the cross-section is the inner bend of the cross-section while the outer is on the right. Solid and dotted lines indicate positive and negative values, respectively. For the small *Re*, $\kappa T^{(1)}$ has a positive value in the semicircle near the inner bend of the pipe and a negative value near the outer wall. When $Re = 20.5$, a negative value

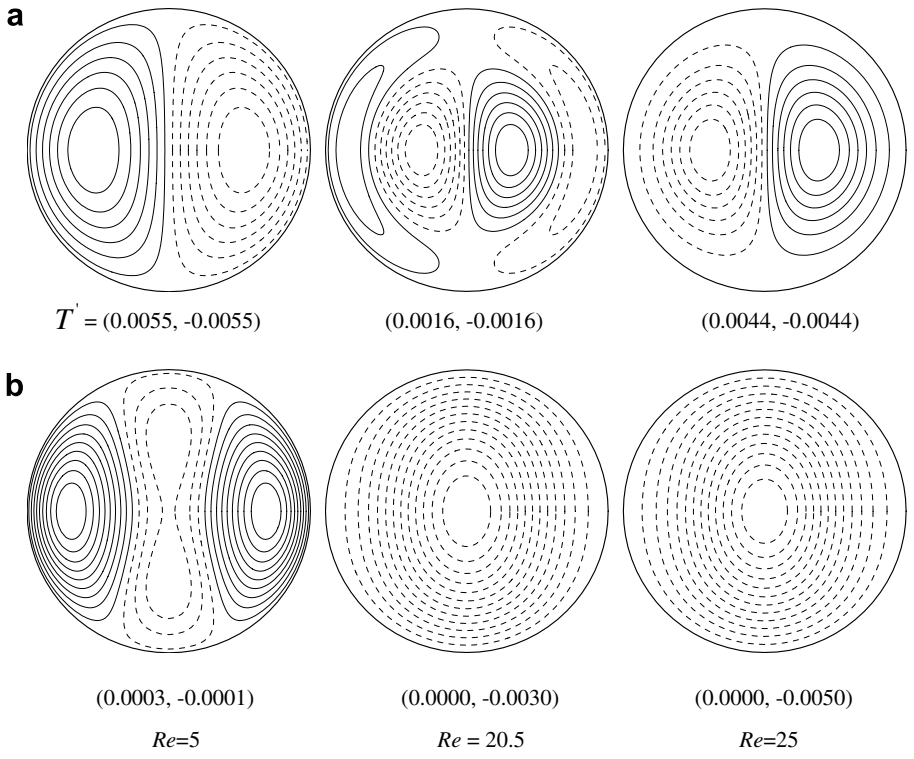

Fig. 2. Temperature distribution of $\kappa T^{(1)}$ and $\kappa^2 T^{(2)}$ ($We = 5, \kappa = 0.1, \frac{\eta_p}{\eta} = 0.2, Pr = 0.85, T'$ =(maximum, minimum); (a) $\kappa T^{(1)}$ and (b) $\kappa^2 T^{(2)}$).

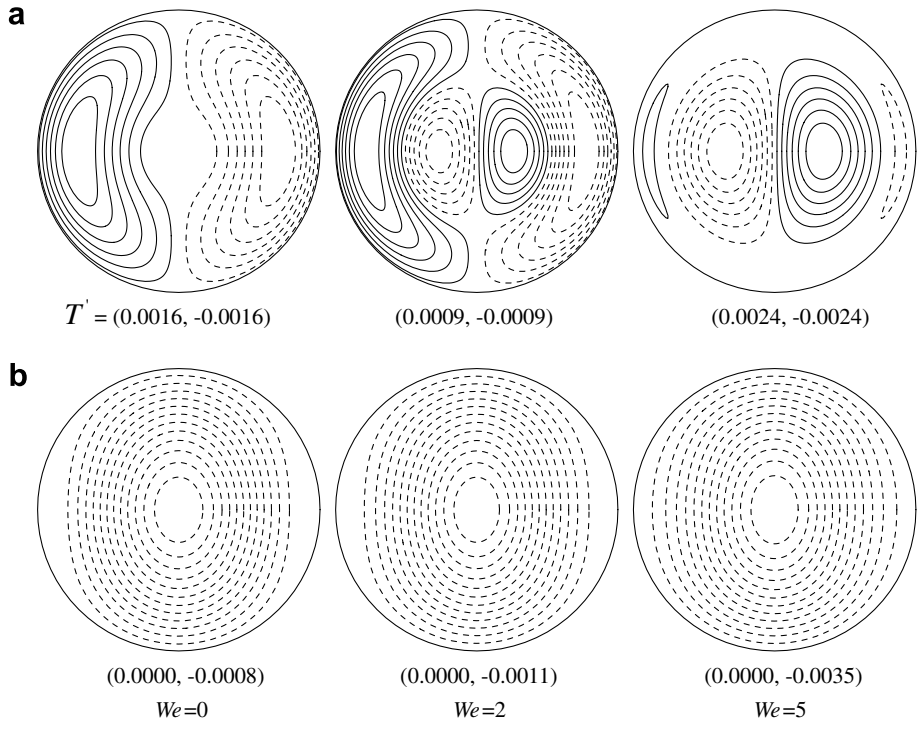

Fig. 3. Temperature distribution of $\kappa T^{(1)}$ and $\kappa^2 T^{(2)}$ ($Re = 22$, $\kappa = 0.1$, $\eta_p/\eta = 0.2$, $Pr = 0.85$, $T^{'}$ = (maximum, minimum); (a) $\kappa T^{(1)}$, (b) $\kappa^2 T^{(2)}$).

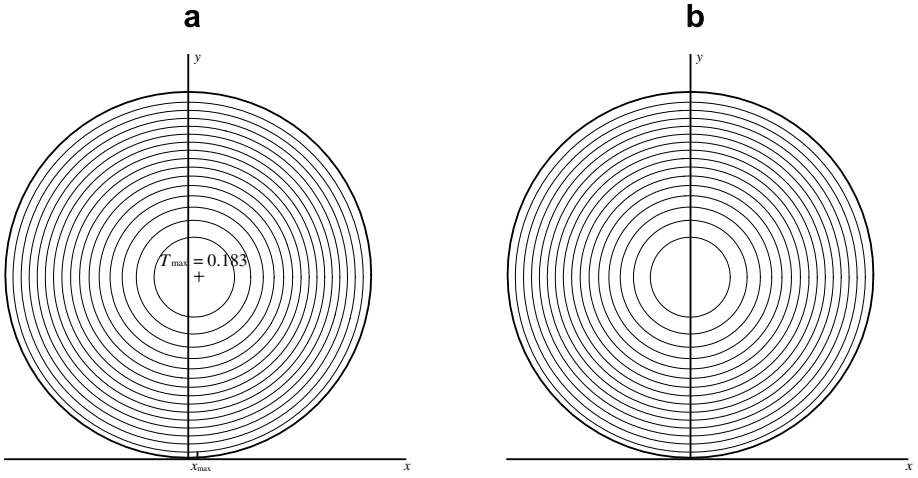

Fig. 4. Contours of temperature for $Re = 25$, $We = 5$, $\kappa = 0.1$, $\eta_p/\eta = 0.2$ and $Pr = 0.85$. (a) $T = T^{(0)} + \kappa T^{(1)} + \kappa^2 T^{(2)}$; (b) $T^{(0)}$.

region appears in the outer half while a positive value region appears near the inner wall. The maximum of $\kappa T^{(1)}$ becomes smaller. As the Re increases to 25, the distribution of $\kappa T^{(1)}$ behaves almost in the same structure as that in the case of $Re = 5$, but a reverse way.

The distribution of $\kappa^2 T^{(2)}$ are as seen in Fig. 2b. For $Re = 5$, a negative value region appears in the center of the pipe while near the outer and inner wall a positive value region appears. When $Re = 20.5$ and $Re = 25$, the negative value region fills the whole cross-section. As Re increases, the absolute value of the minimum of $\kappa^2 T^{(2)}$ becomes larger, while the maximum of $\kappa T^{(1)}$ becomes smaller, so the second order effects be lager than the first order effects.

Fig. 3 shows the distributions of different order solutions of temperature for different We. As seen in Fig. 3, the varieties of distributions of the $\kappa T^{(1)}$ and $\kappa^2 T^{(2)}$ for different We are almost the same as that for different Re. It means that the effects on the temperature distribution of the We are analogous to those of the Re.

Fig. 4 is a representative one of the contours of temperature in curved pipes and the contours of $T^{(0)}$ at the right. Fig. 5 shows the location of maximum in temperature as a function of We. It is useful to investigate the effect of elasticity on the shift. We see in Fig. 5 that similar to the shift of the maximum in axial velocity, for relatively small values of Re, the maximum in temperature is shifted toward the inner bend of the pipe (a negative x_{max}). As either We or Re increases, the inward shift decreases and becomes an outward shift. Fig. 4 is a typical example of the outward shift for a Reynolds number of 25.0, Weissenberg number

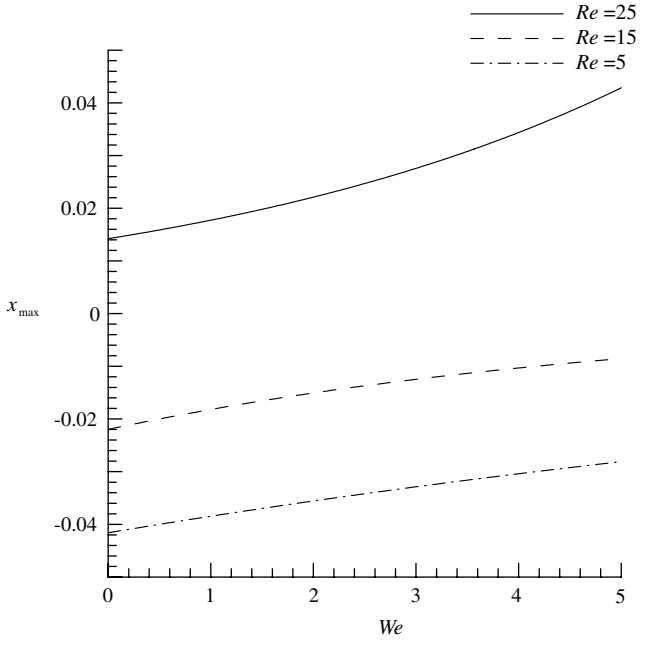

Fig. 5. Location of maximum in temperature as a function of We for $\kappa = 0.1$, $\eta_p/\eta = 0.2$ and $Pr = 0.85$.

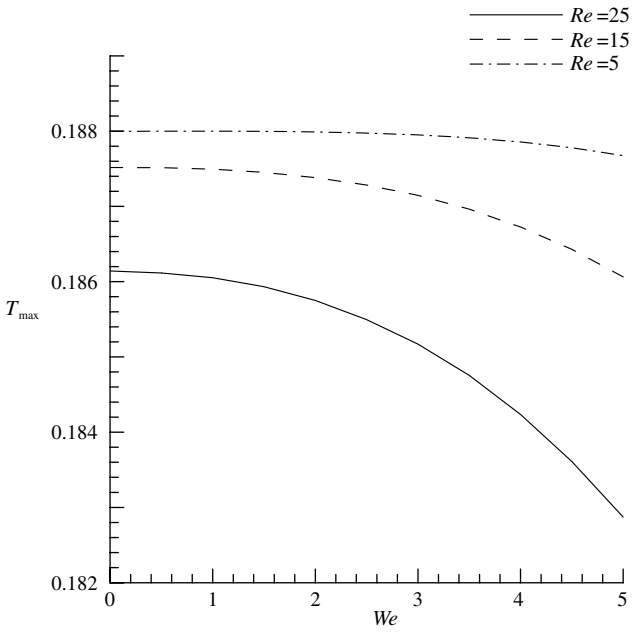

Fig. 6. Variations of T_{max} with We for different values of Re for $\kappa = 0.1$, $\eta_p/\eta = 0.2$ and $Pr = 0.85$.

of 5.0, viscosity ratio of 0.2, curvature ratio of 0.1 and Prandtl number of 0.85. The non-linear interaction of inertia and elasticity results in a greater outward shift than that expected due to adding the independent effects of inertia and elasticity.

Fig. 6 shows the effects of We and Re on T_{max}, which indicates that T_{max} decreases with We or Re increasing. It is because that counter value regions of $\kappa T^{(1)}$ appear when We or Re is large enough as shown in Fig. 2a and Fig. 3a, which decreases the value of $\kappa T^{(1)}$. Meanwhile, the absolute value of the minimum of negative $\kappa^2 T^{(2)}$ becomes larger as shown in Fig. 2b and Fig. 3b. The combined effect of $\kappa T^{(1)}$ and $\kappa^2 T^{(2)}$ decreases T_{max} with We or Re increasing.

4.2. Nusselt number

From reference to the work of Chen and Zhang [10], the non-dimensional peripheral Nusselt number is defined as

$$Nu = \frac{2}{-T_b}\left(\frac{\partial T}{\partial r}\right)_{r=1}, \tag{24}$$

where T_b is the bulk temperature, $T_b = \int_0^1\int_0^{2\pi} Twr\,d\phi\,dr / \int_0^1\int_0^{2\pi} wr\,d\phi\,dr$. The expression of average Nusselt number is defined as the integral of Eq. (24) along the peripheral of pipe,

$$\overline{Nu} = \frac{1}{2\pi}\int_0^{2\pi}\frac{2}{-T_b}\left(\frac{\partial T}{\partial r}\right)_{r=1} d\phi. \tag{25}$$

$\overline{Nu}_0 = 4.3636$ is the value of average Nusselt number is straight pipes, which is independent of any parameters. A measure of the increase in average Nusselt number in a curved pipe relative to that in a straight pipe is defined as

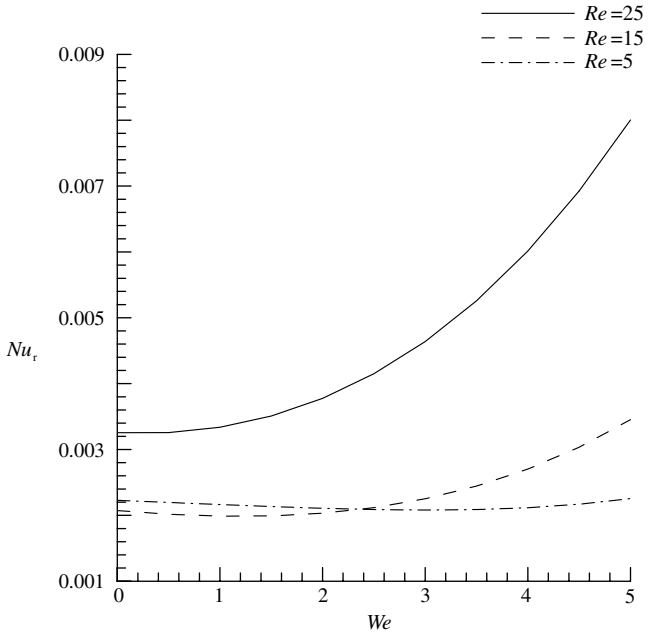

Fig. 7. Variations of Nu_r with We for different values of Re for $\kappa = 0.1$, $\eta_p/\eta = 0.2$ and $Pr = 0.85$.

Table 1
Relative magnitude of terms for different Prandtl numbers

Pe	$We\eta_p/\eta$	$\mathrm{Max}(\lvert T^{(1)}/T^{(0)}\rvert)$	$\mathrm{Max}(\lvert T^{(2)}/T^{(0)}\rvert)$
0.0	1.0	0.5286	2.1803
25.0	1.0	0.3979	2.8631
37.5	1.0	0.7155	3.7987
75.0	1.0	1.7088	8.9827

$$Nu_r = (\overline{Nu} - \overline{Nu}_0)/\overline{Nu}_0 \tag{26}$$

Fig. 7 is the plot of Nu_r against Weissenberg number. For the case of small Reynolds number, Nu_r is almost a constant with respect to variations of Weissenberg number. For $Re = 15$, the Nu_r increases as We increases, while to $Re = 25$, the magnitude of the increase becomes dramatic greater. As the Nusselt number indicates the heat transfer rate of the flow, Fig. 7 shows that the heat transfer rate increases as We increases and the bigger the Re is the greater the magnitude of the increase is. The combined effects of the two parameters result in a greater heat transfer rate than the adding of the two independent effects.

4.3. Range of validity of the perturbation method

There is an implicit assumption in perturbation method that the truncated terms in the perturbation expansion are not significant relative to the terms which are kept. If the coefficients of the expansion, $T^{(0)}$, $T^{(1)}$, $T^{(2)}$, etc., are of order one, then for small perturbation κ the contribution of higher order terms will be negligible. Since the Re and $We\eta_p/\eta$ of the perturbation solutions of w and ψ which are obtained from the work of Robertson and Muller are limited to less than 25 and 1, respectively, the perturbation solutions of T must be under the limit. In order to estimate the range of parameters such as Re, We and η_p/η, the relative size of the terms in the truncated series is considered.

Since the Robertson and Muller have found that the $Re < 25$ and $We\eta_p/\eta < 1$, the only parameter to be discussed here is the Peclet number ($Pe = RePr$). Table 1 displays the relative magnitude of terms in the series solution for different Peclet numbers. Examination of Table 1 reveals that the maximum value of $|T^{(2)}/T^{(0)}|$ becomes significantly larger than order one as the Pe is increasing beyond 37.5. So the Pe of present work's perturbation results is better to less than value of 37.5.

5. Conclusions

The convective heat transfer of Oldroyd-B fluid in curved pipes with circle cross-section is investigated by a perturbation method. The combined effects of viscosity, centrifugal force and elasticity on heat transfer are examine. The major conclusions are drawn as follow:

The zero order perturbation solution of the heat transfer of Oldroyd-B fluid in a curved pipe doesn't depend on any parameters. For the first order and second order cases, both the Re and We affect them. The effects on first order

and second order results of *We* are analogous to those of *Re*. The analysis of the location and value of maximum in temperature indicates that *Re* and *We* affect both of them. The non-linear interaction of inertia and elasticity results in a greater outward shift than that expected due to adding the independent effects of inertia and elasticity. It means that the all of the perturbation solutions determine the value of maximum in temperature, while the first and second order ones affect the location of the maximum as well.

The study of the Nusselt number indicates that the heat transfer rate increases as the *Re* and *We* increases. The combined effects of the two parameters on heat transfer rate are greater than the adding of the two independent ones.

The range of validity of the perturbation method used in present work is examined carefully. To use present work's perturbation result, the values of $We\eta_p/\eta$ and *Pe* are restricted in less than 1 and 37.5, respectively.

Appendix A. Components of the stress tensor in convected coordinates

For fully developed flow, the non-dimensional components of τ^s of convected coordinates are:

$$\begin{aligned}
&\boldsymbol{\tau}^s_{rr} = 2\frac{\eta_s}{\eta}\frac{\partial u}{\partial r}, \quad \boldsymbol{\tau}^s_{r\phi} = \frac{\eta_s}{\eta}\left[\frac{\partial v}{\partial r} + \frac{1}{r}\left(\frac{\partial u}{\partial \phi} - v\right)\right],\\
&\boldsymbol{\tau}^s_{rs} = \frac{\eta_s}{\eta}\left(\frac{\partial w}{\partial r} - \frac{\kappa}{M} w\cos\phi\right),\\
&\boldsymbol{\tau}^s_{\phi\phi} = 2\frac{\eta_s}{\eta}\frac{1}{r}\left(u + \frac{\partial v}{\partial \phi}\right), \quad \boldsymbol{\tau}^s_{\phi s} = \frac{\eta_s}{\eta}\left(\frac{1}{r}\frac{\partial w}{\partial \phi} + \frac{\kappa}{M} w\sin\phi\right),\\
&\boldsymbol{\tau}^s_{ss} = 2\frac{\eta_s}{\eta}\frac{\kappa}{M}(u\cos\phi - v\sin\phi).
\end{aligned} \tag{A.1}$$

The non-dimensional components of $\boldsymbol{\tau}^p$ are:

$$\begin{aligned}
&\boldsymbol{\tau}^p_{rr} + We\left[u\frac{\partial \tau^p_{rr}}{\partial r} + \frac{v}{r}\frac{\partial \tau^p_{rr}}{\partial \phi} - 2\tau^p_{rr}\frac{\partial u}{\partial r} - \frac{2}{r}\tau^p_{r\phi}\frac{\partial u}{\partial \phi}\right]\\
&\quad = 2\frac{\eta_p}{\eta}\frac{\partial u}{\partial r},
\end{aligned} \tag{A.2}$$

$$\begin{aligned}
&\tau^p_{r\phi} + We\left[u\frac{\partial \tau^p_{r\phi}}{\partial r} + \frac{v}{r}\left(\frac{\partial \tau^p_{r\phi}}{\partial \phi} + \tau^p_{rr}\right)\right.\\
&\quad \left. - \tau^p_{r\phi}\frac{\partial u}{\partial r} - \frac{\tau^p_{\phi\phi}}{r}\frac{\partial u}{\partial \phi} - \tau^p_{rr}\frac{\partial v}{\partial r} - \frac{\tau^p_{r\phi}}{r}\left(u + \frac{\partial v}{\partial \phi}\right)\right]\\
&\quad = \frac{\eta_p}{\eta}\left[\frac{\partial v}{\partial r} + \frac{1}{r}\left(\frac{\partial u}{\partial \phi} - v\right)\right],
\end{aligned} \tag{A.3}$$

$$\begin{aligned}
&\tau^p_{rs} + We\left[u\frac{\partial \tau^p_{rs}}{\partial r} + \frac{v}{r}\frac{\partial \tau^p_{rs}}{\partial \phi} - \tau^p_{rs}\frac{\partial u}{\partial r} - \frac{\tau^p_{\phi s}}{r}\frac{\partial u}{\partial \phi} - \tau^p_{rr}\frac{\partial w}{\partial r} - \frac{\tau^p_{r\phi}}{r}\frac{\partial w}{\partial \phi}\right.\\
&\quad \left. + \frac{\kappa}{M}\left(\tau^p_{rs}(-u\cos\phi + v\sin\phi) + w\tau^p_{rr}\cos\phi - w\tau^p_{r\phi}\sin\phi\right)\right]\\
&\quad = \frac{\eta_p}{\eta}\left(\frac{\partial w}{\partial r} - \frac{\kappa}{M} w\cos\phi\right),
\end{aligned} \tag{A.4}$$

$$\begin{aligned}
&\tau^p_{\phi\phi} + We\left[u\frac{\partial \tau^p_{\phi\phi}}{\partial r} + \frac{v}{r}\left(\frac{\partial \tau^p_{rr}}{\partial \phi} + 2\tau^p_{r\phi}\right) - 2\tau^p_{r\phi}\frac{\partial v}{\partial r} - \frac{2}{r}\tau^p_{\phi\phi}\left(u + \frac{\partial v}{\partial \phi}\right)\right]\\
&\quad = \frac{2}{r}\frac{\eta_p}{\eta}\left(u + \frac{\partial v}{\partial \phi}\right),
\end{aligned} \tag{A.5}$$

$$\begin{aligned}
&\tau^p_{\phi s} + We\left[u\frac{\partial \tau^p_{\phi s}}{\partial r} + \frac{v}{r}\left(\frac{\partial \tau^p_{rs}}{\partial \phi} + \tau^p_{rs}\right) - \tau^p_{rs}\frac{\partial v}{\partial r} - \frac{\tau^p_{\phi s}}{r}\left(u + \frac{\partial v}{\partial \phi}\right)\right.\\
&\quad - \tau^p_{r\phi}\frac{\partial w}{\partial r} - \frac{\tau^p_{\phi\phi}}{r}\frac{\partial w}{\partial \phi} + \frac{\kappa}{M}\left(\tau^p_{\phi s}(-u\cos\phi + v\sin\phi)\right.\\
&\quad \left.\left. + w\tau^p_{r\phi}\cos\phi - w\tau^p_{\phi\phi}\sin\phi\right)\right]\\
&\quad = \frac{\eta_p}{\eta}\left(\frac{1}{r}\frac{\partial w}{\partial \phi} + \frac{\kappa}{M} w\sin\phi\right),
\end{aligned} \tag{A.6}$$

$$\begin{aligned}
&\tau^p_{ss} + We\left[u\frac{\partial \tau^p_{ss}}{\partial r} + \frac{v}{r}\frac{\partial \tau^p_{ss}}{\partial \phi} - 2\tau^p_{rs}\frac{\partial w}{\partial r} - \frac{2}{r}\tau^p_{\phi s}\frac{\partial w}{\partial \phi}\right.\\
&\quad \left. + 2\frac{\kappa}{M}(\tau^p_{ss}(-u\cos\phi + v\sin\phi) + w\tau^p_{rs}\cos\phi - w\tau^p_{\phi s}\sin\phi)\right]\\
&\quad = 2\frac{\eta_p}{\eta}\frac{\kappa}{M}(u\cos\phi - v\sin\phi).
\end{aligned} \tag{A.7}$$

Appendix B. Perturbation solution of $T^{(2)}$

The second term in the series solution for the temperature takes the form $T^{(2)} = g_2(r) + \cos(2\phi)g_3(r)$, where:

$$\begin{aligned}
g_2(r) = &\left(\frac{1}{64} + \frac{7}{96}r^2 - \frac{17}{128}r^4 + \frac{17}{384}r^6\right)\\
&+ Re^2\left(-\frac{581}{4423680} + \frac{371}{2764800}r^2 + \frac{1}{20480}r^4 - \frac{1}{12288}r^6 + \frac{11}{294912}r^8 - \frac{1}{122880}r^{10} + \frac{1}{1843200}r^{12}\right)\\
&+ Re^4\left(-\frac{4741147}{42138206208000} + \frac{1373}{4954521600}r^2 - \frac{19}{53084160}r^4 + \frac{331}{955514880}r^6 - \frac{11}{47185920}r^8 + \frac{569}{5308416000}r^{10}\right.\\
&\left. - \frac{157}{4777574400}r^{12} + \frac{11}{1734082560}r^{14} - \frac{1}{1486356480}r^{16} + \frac{1}{34398535680}r^{18}\right)\\
&+ We\frac{\eta_p}{\eta}\left[Re\left(\frac{889}{552960} - \frac{389}{69120}r^2 + \frac{37}{4608}r^4 - \frac{79}{13824}r^6 + \frac{215}{110592}r^8 - \frac{11}{46080}r^{10}\right)\right.
\end{aligned}$$

$$+Re^3\left(-\frac{127501}{156067430400}+\frac{13397}{2786918400}r^2-\frac{1}{92160}r^4+\frac{517}{39813120}r^6-\frac{2951}{318504960}r^8+\frac{541}{132710400}r^{10}-\frac{431}{398131200}r^{12}\right.$$
$$\left.+\frac{151}{975421440}r^{14}-\frac{13}{1486356480}r^{16}\right)\Big]+We^2\frac{\eta_p}{\eta}\left[\frac{\eta_p}{\eta}\left(\frac{217}{13824}-\frac{5}{128}r^2+\frac{1}{24}r^4-\frac{41}{1728}r^6+\frac{25}{4608}r^8\right)\right.$$
$$+Re^2\left(-\frac{7313}{101606400}+\frac{233}{1658880}r^2-\frac{1}{9216}r^4+\frac{1}{20736}r^6-\frac{1}{165888}r^8-\frac{1}{307200}r^{10}+\frac{1}{829440}r^{12}-\frac{1}{8128512}r^{14}\right)$$
$$\left.+Re^2\frac{\eta_p}{\eta}\left(\frac{444191}{9754214400}-\frac{13}{368640}r^2-\frac{49}{552960}r^4+\frac{817}{4976640}r^6-\frac{341}{2654208}r^8+\frac{97}{1843200}r^{10}-\frac{1}{92160}r^{12}+\frac{71}{81285120}r^{14}\right)\right]$$
$$+We^3\left(\frac{\eta_p}{\eta}\right)^2\left[Re\left(-\frac{1457}{1244160}+\frac{59}{34560}r^2-\frac{11}{23040}r^4-\frac{29}{155520}r^6+\frac{7}{46080}r^8-\frac{1}{34560}r^{10}+\frac{1}{207360}r^{12}\right)\right.$$
$$\left.+Re\frac{\eta_p}{\eta}\left(\frac{763}{1382400}-\frac{49}{69120}r^2-\frac{1}{4608}r^4+\frac{35}{41472}r^6-\frac{37}{55296}r^8+\frac{13}{57600}r^{10}-\frac{11}{414720}r^{12}\right)\right]$$
$$+We^4\left(\frac{\eta_p}{\eta}\right)^3\left[\left(-\frac{61}{21600}+\frac{1}{192}r^2-\frac{1}{288}r^4+\frac{1}{864}r^6-\frac{1}{14400}r^{10}\right)+\frac{\eta_p}{\eta}\left(\frac{107}{64800}-\frac{1}{432}r^2+\frac{1}{648}r^6-\frac{1}{864}r^8+\frac{1}{3600}r^{10}\right)\right]$$
$$+Pr\left[Re^2\left(\frac{7877}{66355200}-\frac{863}{1105920}r^2+\frac{13}{8192}r^4-\frac{499}{331776}r^6+\frac{653}{884736}r^8-\frac{161}{921600}r^{10}+\frac{17}{1105920}r^{12}\right)\right.$$
$$+Re^4\left(-\frac{58721}{802632499200}+\frac{73}{199065600}r^2-\frac{409}{530841600}r^4+\frac{4241}{4777574400}r^6-\frac{989}{1592524800}r^8+\frac{37}{132710400}r^{10}\right.$$
$$\left.\left.-\frac{263}{3185049600}r^{12}+\frac{29}{1857945600}r^{14}\frac{7}{4246732800}r^{16}+\frac{1}{14332723200}r^{18}\right)\right]$$
$$+PrWe\frac{\eta_p}{\eta}\left[Re\left(\frac{1027}{1382400}-\frac{217}{46080}r^2+\frac{83}{9216}r^4-\frac{53}{6912}r^6+\frac{19}{6144}r^8-\frac{107}{230400}r^{10}\right)\right.$$
$$+Re^3\left(-\frac{45509}{22295347200}+\frac{1}{97200}r^2-\frac{641}{29491200}r^4+\frac{1249}{49766400}r^6-\frac{5533}{318504960}r^8+\frac{247}{33177600}r^{10}-\frac{1547}{796262400}r^{12}\right.$$
$$\left.\left.+\frac{193}{696729600}r^{14}-\frac{17}{1061683200}r^{16}\right)\right]+Pr\left(We\frac{\eta_p}{\eta}\right)^2Re^2\left(-\frac{989}{58060800}+\frac{281}{3317760}r^2-\frac{581}{3317760}r^4+\frac{647}{3317760}r^6\right.$$
$$\left.-\frac{7}{55296}r^8+\frac{799}{16588800}r^{10}-\frac{11}{1105920}r^{12}+\frac{19}{23224320}r^{14}\right)+Pr\left(We\frac{\eta_p}{\eta}\right)^3Re\left(-\frac{37}{829440}+\frac{1}{4608}r^2-\frac{1}{2304}r^4+\frac{19}{41472}r^6\right.$$
$$\left.-\frac{5}{18432}r^8+\frac{1}{11520}r^{10}-\frac{1}{82944}r^{12}\right)+Pr^2Re^4\left(-\frac{97207}{401316249600}+\frac{103}{79626240}r^2-\frac{629}{212336640}r^4+\frac{1829}{477757440}r^6\right.$$
$$\left.-\frac{3943}{1274019840}r^8+\frac{289}{176947200}r^{10}-\frac{179}{318504960}r^{12}+\frac{89}{743178240}r^{14}-\frac{1}{70778880}r^{16}+\frac{1}{1433272320}r^{18}\right)$$
$$+Pr^2We\frac{\eta_p}{\eta}Re^3\left(-\frac{34163}{11147673600}+\frac{211}{13271040}r^2-\frac{929}{26542080}r^4+\frac{341}{79626240}r^6-\frac{851}{26542080}r^8+\frac{503}{33177600}r^{10}\right.$$
$$\left.-\frac{11}{2488320}r^{12}+\frac{11}{15482880}r^{14}-\frac{1}{21233664}r^{16}\right)+Pr^2\left(We\frac{\eta_p}{\eta}\right)^2Re^2\left(-\frac{563}{58060800}+\frac{1}{20480}r^2-\frac{19}{184320}r^4+\frac{197}{1658880}r^6\right.$$
$$\left.-\frac{1}{12288}r^8+\frac{31}{921600}r^{10}-\frac{13}{1658880}r^{12}+\frac{1}{1290240}r^{14}\right). \tag{A.8}$$

$$g_3(r)=\left(\frac{149}{1536}r^2-\frac{55}{384}r^4+\frac{71}{1536}r^6\right)$$
$$+Re^2\left(-\frac{12017}{116121600}r^2+\frac{187}{829440}r^4-\frac{409}{2211840}r^6+\frac{73}{921600}r^8-\frac{13}{7372800}r^{10}+\frac{53}{38707200}r^{12}\right)$$
$$+Re^4\left(\frac{47801}{1123685498880}r^2-\frac{14569}{140460687360}r^4+\frac{2297}{22295347200}r^6-\frac{439}{7431782400}r^8+\frac{139}{6370099200}r^{10}-\frac{61}{11147673600}r^{12}\right.$$

$$+\frac{29}{29727129600}r^{14}-\frac{47}{468202291200}r^{16}+\frac{1}{234101145600}r^{18}\Big)+We\frac{\eta_p}{\eta}\Big[Re\Big(-\frac{173}{92160}r^2+\frac{613}{138240}r^4-\frac{353}{92160}r^6$$
$$+\frac{5}{3456}r^8-\frac{1}{5760}r^{10}\Big)+Re^3\Big(\frac{329437}{117050572800}r^2-\frac{5683}{796262400}r^4+\frac{2281}{309657600}r^6-\frac{11881}{2786918400}r^8+\frac{1}{655360}r^{10}$$
$$-\frac{13}{37158912}r^{12}+\frac{1}{21772800}r^{14}-\frac{283}{117050572800}r^{16}\Big)\Big]+We^2\frac{\eta_p}{\eta}\Big[\frac{\eta_p}{\eta}\Big(-\frac{119}{8640}r^2+\frac{55}{1728}r^4-\frac{29}{1152}r^6+\frac{41}{5760}r^8\Big)$$
$$+Re^2\frac{\eta_p}{\eta}\Big(\frac{78181}{1393459200}r^2-\frac{10853}{69672960}r^4+\frac{1}{5670}r^6-\frac{587}{5529600}r^8+\frac{13}{368640}r^{10}-\frac{121}{19353600}r^{12}+\frac{41}{92897280}r^{14}\Big)$$
$$+Re^2\Big(\frac{25}{2064384}r^2-\frac{113}{7741440}r^4-\frac{1}{122880}r^6+\frac{101}{5529600}r^8-\frac{7}{737280}r^{10}+\frac{13}{6451200}r^{12}-\frac{1}{6193152}r^{14}\Big)\Big]$$
$$+We^3\Big(\frac{\eta_p}{\eta}\Big)^2\Big[Re\Big(\frac{391}{1935360}r^2-\frac{1}{4608}r^4-\frac{19}{92160}r^6+\frac{9}{25600}r^8-\frac{1}{6912}r^{10}+\frac{23}{1612800}r^{12}\Big)$$
$$+Re\frac{\eta_p}{\eta}\Big(\frac{4313}{9676800}r^2-\frac{271}{207360}r^4+\frac{47}{30720}r^6-\frac{307}{345600}r^8+\frac{101}{414720}r^{10}-\frac{29}{1209600}r^{12}\Big)\Big]$$
$$+We^4\Big(\frac{\eta_p}{\eta}\Big)^3\Big[\Big(\frac{11}{17280}r^2-\frac{1}{2160}r^4-\frac{13}{11520}r^6+\frac{1}{720}r^8-\frac{1}{2304}r^{10}\Big)+\frac{\eta_p}{\eta}\Big(\frac{17}{12960}r^2-\frac{5}{1296}r^4+\frac{19}{4320}r^6-\frac{1}{432}r^8+\frac{1}{2160}r^{10}\Big)\Big]$$
$$+Pr\Big[Re^2\Big(-\frac{4063}{25804800}r^2+\frac{223}{552960}r^4-\frac{77}{184320}r^6+\frac{1247}{5529600}r^8-\frac{131}{2211840}r^{10}+\frac{109}{19353600}r^{12}\Big)$$
$$+Re^4\Big(\frac{268679}{891813888000}r^2-\frac{199}{232243200}r^4+\frac{90373}{89181388800}r^6-\frac{18359}{27869184000}r^8+\frac{1}{3932160}r^{10}-\frac{233}{3715891200}r^{12}$$
$$+\frac{307}{29727129600}r^{14}-\frac{11}{11147673600}r^{16}+\frac{29}{891813888000}r^{18}\Big)\Big]+PrWe\frac{\eta_p}{\eta}\Big[Re\Big(-\frac{229}{92160}r^2+\frac{85}{13824}r^4-\frac{71}{12288}r^6$$
$$+\frac{35}{13824}r^8-\frac{77}{184320}r^{10}\Big)+Re^3\Big(\frac{135169}{13005619200}r^2-\frac{84869}{2786918400}r^4+\frac{833}{22118400}r^6-\frac{24071}{928972800}r^8+\frac{841}{79626240}r^{10}$$
$$-\frac{481}{185794560}r^{12}+\frac{1993}{5573836800}r^{14}-\frac{401}{19508428800}r^{16}\Big)\Big]+PrWe^2\frac{\eta_p}{\eta}Re^2\Big[\Big(\frac{7613}{309657600}r^2-\frac{1}{23040}r^4+\frac{1}{184320}r^6$$
$$+\frac{23}{691200}r^8-\frac{13}{491520}r^{10}+\frac{23}{3225600}r^{12}-\frac{1}{1769472}r^{14}\Big)+\frac{\eta_p}{\eta}\Big(\frac{34319}{348364800}r^2-\frac{1471}{4976640}r^4+\frac{619}{1658880}r^6-\frac{1061}{4147200}r^8$$
$$+\frac{97}{995328}r^{10}-\frac{223}{11612160}r^{12}+\frac{1}{663552}r^{14}\Big)\Big]+PrWe^3\Big(\frac{\eta_p}{\eta}\Big)^2Re\Big[\Big(\frac{181}{1612800}r^2-\frac{1}{5760}r^4-\frac{1}{30720}r^6+\frac{11}{57600}r^8-\frac{11}{92160}r^{10}$$
$$+\frac{1}{44800}r^{12}\Big)+\frac{\eta_p}{\eta}\Big(\frac{1283}{4147200}r^2-\frac{1}{1080}r^4+\frac{317}{276480}r^6-\frac{769}{1036800}r^8+\frac{101}{414720}r^{10}-\frac{11}{345600}r^{12}\Big)\Big]$$
$$+Pr^2Re^4\Big(-\frac{533}{33443020800}r^2-\frac{11}{318504960}r^4+\frac{131}{637009920}r^6-\frac{497}{1592524800}r^8\frac{299}{1274019840}r^{10}-\frac{61}{619315200}r^{12}$$
$$+\frac{1}{42467328}r^{14}-\frac{1}{334430208}r^{16}+\frac{1}{6370099200}r^{18}\Big)+Pr^2We\frac{\eta_p}{\eta}Re^3\Big(-\frac{127}{1393459200}r^2-\frac{31}{39813120}r^4+\frac{31}{10616832}r^6$$
$$-\frac{191}{49766400}r^8+\frac{67}{26542080}r^{10}-\frac{41}{46448640}r^{12}+\frac{5}{31850496}r^{14}-\frac{1}{92897280}r^{16}\Big)$$
$$+Pr^2\Big(We\frac{\eta_p}{\eta}\Big)^2Re^2\Big(\frac{37}{464486400}r^2-\frac{1}{276480}r^4+\frac{23}{2211840}r^6-\frac{1}{82944}r^8+\frac{23}{3317760}r^{10}-\frac{19}{9676800}r^{12}+\frac{1}{4423680}r^{14}\Big). \tag{A.9}$$

References

[1] W.R. Dean, Note on the motion of fluid in a curved pipe, Phil. Mag. 7 (4) (1927) 208–223.

[2] W.R. Dean, The stream-line motion of fluid in a curved pipe, Phil. Mag. 7 (5) (1928) 673–695.

[3] M. Akiyama, K.C. Cheng, Boundary vorticity method for laminar forced convected heat transfer in curved pipe, Int. J. Heat Mass Transfer 14 (1971) 1659–1675.

[4] S.V. Patankar, V.S. Pratap, D.B. Spalding, Prediction of laminar flow and heat transfer in helically coiled pipes, J. Fluid Mech. 62 (1974) 539–551.

[5] W.J. Yang, S.F. Chang, Combined free and forced convection for developed flow in curved pipes with finite curvature ratio, Int. J. Heat Mass Transfer 15 (6) (1994) 470–476.
[6] S. Garimella, D.E. Chdrards, Experimental investigation of heat transfer in coiled annular ducts, J. Heat Transfer 110 (1988) 329–336.
[7] G. Yang, M.A. Ebadian, Convective heat transfer in a curved annular-sector duct, J. Thermophys. Heat Transfer 7 (3) (1993) 441–446.
[8] G. Yang, M.A. Ebadian, Effect of torsion on heat transfer in the curved annular sector duct, J. Thermophys. Heat Transfer 8 (3) (1994) 580–586.
[9] Y.D. Choi, S.O. Park, Mixed convection flow in curved annular ducts, Int. J. Heat Mass Transfer 37 (17) (1994) 2761–2769.
[10] H.J. Chen, B.Z. Zhang, J.F. Ma, Theoretical and numerical analysis of convective heat transfer in rotation helical pipes, Int. J. Heat Mass Transfer 46 (2003) 4899–4909.
[11] H.J. Chen, B.Z. Zhang, Fluid flow and mixed convection heat transfer in a rotating curved pipe, Int. J. Therm. Sci. 42 (2003) 1047–1059.
[12] A.M. Robertson, S.J. Muller, Flow of Oldroyd-B fluids in curved pipes of circular and annular cross-section, J. Non-linear Mech. 31 (1) (1996) 1–20.
[13] W. Jitchote, A.M. Robertson, Flow of second order fluids in curved pipes, J. Non-Newtonian Fluid Mech. 90 (2000) 91–116.
[14] Y.R. Fan, R.I. Tanner, N. Phan-Thien, Fully developed viscous and viscoelastic flows in curved pipes, J. Fluid Mech. 440 (2001) 327–357.
[15] Y.I. Cho, J.P. Hartnett, Non-Newtonian fluids in circular pipe flow, Advance in Heat Transfer, vol. 15, Academic Press, New York, 1982.
[16] K.H. Toh, A.J. Ghajar, Heat transfer in thermal entrance region for viscoelastic fluids in turbulent pipe flows, Int. J. Heat Mass Transfer 31 (1988) 1261–1268.
[17] F.T. Pinho, P.J. Oliveira, Analysis of forced convection in pipes and channels with the simplified Phan-Thien–Tanner fluid, Int. J. Heat Mass Transfer 43 (2000) 2273–2287.
[18] C.J. Bolinder, Curvilinear coordinates and physical components: an application to the problem of viscous flow and heat transfer in smoothly curved ducts, J. Appl. Mech. 63 (1996) 985–989.